Journal of Polymers and the Environment (2022) 30:5313–5326
https://doi.org/10.1007/s10924-022-02588-x

ORIGINAL PAPER

Effect of Extracted Nano-cellulose from Paper Egg Trays on Mechanical Properties of Vinyl Ester/Kenaf Fibers Composites

Ruiwen Yu[1] · M.N. Prabhakar[2] · Jung-il Song[3]

Accepted: 7 September 2022 / Published online: 17 October 2022

Abstract

This study sustainably developed natural fiber composites from extracted nano-cellulose (ENC) from waste paper egg trays and incorporated them into vinyl ester/kenaf fiber (ENCVK) composites using a vacuum-assisted resin transfer molding (VARTM) process. Overhead stirring, three-roll milling, and ultrasonication were used to uniformly mix the ENC into the resin. The surface morphology exhibited a homogeneous distribution of ENC in the composites, and change in the % of transmittance of spectral peaks refers to the chemical interaction of ENC with the VK composites. ENC significantly improved tensile (32 MPa), flexural (77 MPa) and impact (0.0197 J/mm^2) properties of the VK composites (18 MPa, 61 MPa and 0.009 J/mm^2) by approximately 73%, 25% and 110%, respectively. Further, ENC inclusion enhanced the storage modulus of VK composites owing to the addition of rigid ENC particles, which enhances the bearing capacity of the composite and is reflected in its high performance. The loss modulus indicates that the interfacial interaction of ENCVK is more vital than VK. The tan Δ value indicates that the filler has strong adhesion, and the polymer cohesion damping is reduced, thus reflecting its high performance.

Keywords Nano-cellulose · Kenaf fiber · Vinyl ester · Polymer composites · Mechanical properties

Introduction

The scientific and industrial communities have been eagerly awaiting renewable, biodegradable, and environmentally friendly materials due to several cautious environmental issues created by societal development. Traditional polymers are driving factors that threaten ecology, contributing to global warming and holes in the ozone layer. Because traditional polymers take decades to decompose and during this process the additives added in manufacturing process responsible for releasing large quantities of chlorofluorocarbons, carbon tetrachloride, methyl chloroform, halons, etc., [1, 2]. Cellulose is the most abundant renewable polymer on Earth, and more than 100 billion tons are produced by nature every year. Plants (lignocellulose) are the primary source of cellulose, and their percentage depends mainly on their origin and environmental conditions [3]. Over the past decade, the application of nanostructured cellulose in composite materials has become a popular research topic owing to its specific chemical and physical properties. Nanocellulose has been extracted from lignocellulosic fibers, such as crude oil palm leaves [4], cotton fiber [5], bagasse [6], and jute fibers [7].

Polymers have high specific strength and good mechanical properties, but the performance of fibers far exceeds that of polymers; thus, they are used as reinforcing materials to improve the mechanical properties of polymers. Polymers have insufficient thermal stability, and fiber reinforcement can result in a wide range of fiber-reinforced polymer

✉ M.N. Prabhakar
dr_prabhakar@changwon.ac.kr

✉ Jung-il Song
jisong@changwon.ac.kr

Ruiwen Yu
ruiwen0731@gmail.com

[1] Department of Smart Manufacturing Engineering, Changwon National University, Uichang-gu, Changwon, Gyeongsangnam-do 51140, Republic of Korea

[2] Research Institute of Mechatronics, Department of Mechanical Engineering, Changwon National University, Uichang-gu, Changwon, Gyeongsangnam-do 51140, Republic of Korea

[3] Department of Mechanical Engineering, Changwon National University, Uichang-gu, Changwon, Gyeongsangnam-do 51140, Republic of Korea

applications in the thermal field. Thermoplastics and thermosets are the two main types of polymers, and they have labile extensible and flexible structures. Thermoplastic polymers exhibit poor mechanical properties, which can be resolved by using fiber-reinforced polymers. A cellulose-reinforced polymer is a composite material that mechanically enhances the strength and elasticity of the polymer because it provides strength and stiffness to the composite material in one direction, whereby the reinforcement bears loads along the length of the fiber. However, the strength and deformation of cellulose-reinforced materials decreases and increases, respectively, at high temperatures, and shock loads can destroy these materials during impact loading.

Nano-cellulose has recently been used as a supportive reinforcement for manufacturing synthetic/natural fiber polymer composites, and the resultant composites are widely used in automobiles, construction electronics, and medicinal applications [8, 9]. The nano-cellulose surface must be modified if it is used as a reinforcement to (carbon fiber reinforced polymers) CFRP or (glass fiber reinforced polymers) GFRP composites to improve the compatibility between the matrix and fiber the treatment should not damage the natural cellulose structure [10, 11]. However, the properties of natural fiber-reinforced polymer composites depend on several factors, including fiber chemical composition, unit cell size, microfibril angles, defects, structure, physical and mechanical properties, and fiber-polymer interactions [12]. Nano-cellulose-reinforced natural fiber composites have three bonding interactions, namely (1) strong mechanical interaction between natural fiber and matrix, (2) weak mechanical interaction between nano-cellulose and natural fiber, and (3) bonding between nano-cellulose and matrix [11, 13]. Moreover, the properties of the composites depend on the cellulosic content of the fibers.

Mohammadkazemi et al. studied the effects of bacterial nano-cellulose as a powder, gel, and coated onto the fibers on the mechanical and microstructural properties of bagasse fiber–cement composites [14]. Tang et al. investigated novel nano-composites of nano-cellulose or whiskers combined with epoxy resins [15]. Wang et al. chemically modified cellulose nano-whiskers with dodecenyl succinic anhydride to obtain hydrophobic nano-whiskers with enhanced thermosetting epoxy polymer properties [16]. Gan et al. studied plant-based nano-cellulose composites and their properties and determined the effect of nano-cellulose incorporation on the thermodynamic and dynamic mechanical properties of nano-cellulose composites [17]. Ferreira et al. studied the use of natural fillers (natural fibers, cellulose nano-crystals, and nano-fibrillated cellulose) as reinforcements in polymer composites for the automotive industry [18].

This study focused on reinforcing the inexpensive ENC into VE/KF composites through the vacuum-assisted resin transfer molding (VARTM) process, evaluating the impact of ENC on the mechanical behavior of fabricated composites, and comparing it with CMC-loaded VE/KF composites. The mixing process included overhead stirring, three-roll milling, and ultrasonication for better dispersion of ENC in the matrix and the homogeneous dispersion of the composites. The basic properties of the composites were studied by characterizing using scanning electron microscopy (SEM), Fourier transform infrared spectroscopy (FTIR), X-ray diffraction (XRD), and thermogravimetric analysis (TGA), and the mechanical properties were determined using a universal testing instrument (UTM) and by dynamic mechanical analysis (DMA). Additionally, the properties of the ENC-reinforced VE/KF composites were compared with those of commercial nano-cellulose reinforced VE/KF composites.

Experimental Methods

Materials

Sodium hydroxide (NaOH), Sulfuric acid (H_2SO_4) purchased from Samchun Pure Chemical Co., LTD. Korea. Waste paper egg trays (30-egg package) are gathered from university campus. Vinyl ester (KRF-1031 and density 1.03 g/cm^3) is purchased from CCP Composites, Korea. Kenaf fibers (bi-directional) were procured from Sungchang Industries, Korea. Commercial Nano-cellulose was obtained from ANPOLY Co., LTD, Korea. Deionized water were used for the experimentation.

Fabrication Process

Extraction of Nano-cellulose

The collected egg trays were washed under running water and dried at room temperature. The dried egg trays were cut into small pieces using scissors. Small pieces of egg trays were immersed in 1 L of 2 wt% NaOH solution and mixed by an overhead stirrer at 400 rpm at ambient temperature for 4 h. The resulting suspension was cleaned with DI water until it was neutralized (pH 7), and was then dried in an oven (Fleta 5, LK LAB Co., LTD, Republic of Korea) at 60 °C. Acid hydrolysis was performed at ambient temperature and at a stirring speed of 400 rpm for 1 h using a 50 wt% H_2SO_4 solution. The resultant precipitate was cleaned using a centrifuge (Fleta 5, Hanil Scientific Inc., Republic of Korea) with DI water until neutralized (pH 7). The wet extracted dough was placed in an oven at 60 °C for complete drying. The dried agglomerated dough was subjected to a mechano-ball mill (Dongwon Scientific Co., Korea) at 130 rpm for 4 h to obtain nano-cellulose, as discussed in our recent publication [19].

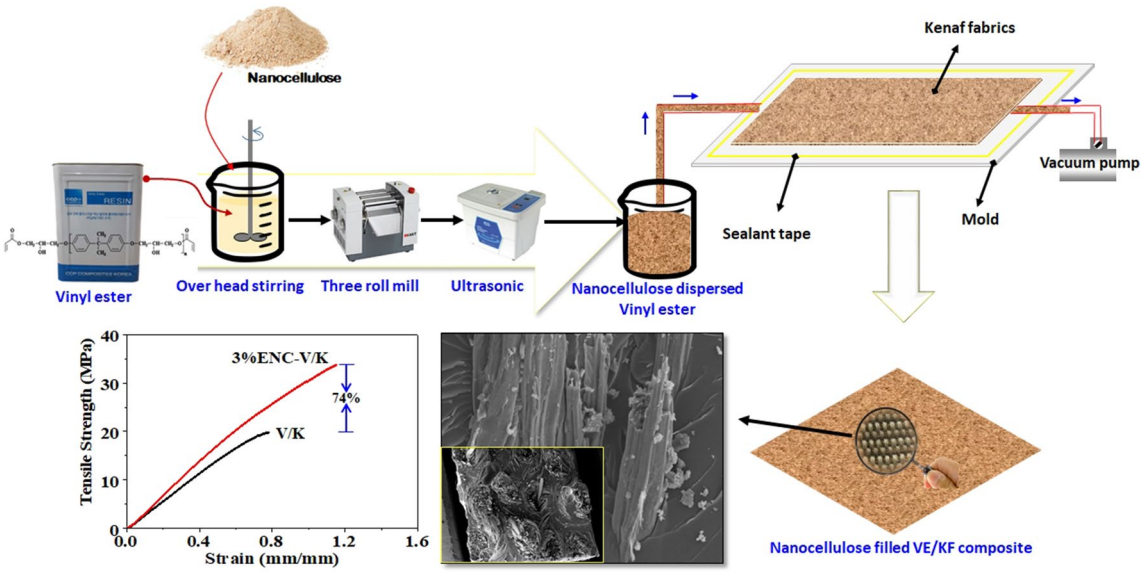

Scheme 1 Schematic representation of the nano-cellulose kenaf fiber vinyl ester composites preparation process

Preparation of ENCV Resin by Mechanical Mixing

The mixing of nano-cellulose with resin was done with three important mechanical process such as overhead stirring, three-roll mill and ultra-sonication. The various % (1, 2, 3, and 4) of extracted nano-cellulose mixed with 600 ml vinyl ester resin, stirred at 450 rpm for 4 h, followed by three-roll mill (75 rpm) for 2 times. The mixed resin was collected and finally sonicated (42 KHZ ± 6%) for 1 h. Similar procedure was followed for mixing of commercial nano-cellulose (2 and 3%) into VE resin.

Manufacturing of the Vinyl Ester/Kenaf Fiber (ENCVK) Composite

The Kenaf fabrics were modified with a 2% alkali solution to remove surface impurities and storage chemicals before using them for composite manufacturing. The ENCVK composites were manufactured using VARTM. First, a Teflon sheet was placed on an aluminum plate to avoid sticking of the final composites. Six layers of kenaf fabrics (300 × 300 mm^2) were laid on the mold and the fabric layers were covered with a peel ply, followed by a resin flow net. Finally, a sealing tape was placed around the fabrics. The resin inlet and outlet were connected to a mold using hoses. A constant vacuum pressure of 0.07 MPa was maintained during the vacuum process. The outlet hose was connected to a vacuum pump, and the inlet hose was connected to the resin solution. First, the vacuum pump removed the gas from the mold while maintaining a constant vacuum pressure to allow the resin to enter the mold. The prepared composite material was cured in a curing oven at 60 °C for 6 h. A similar procedure was followed for the manufacture of pure composites (Scheme 1). The specimens were tested against ASTM test standards [20–22]. The density and void content of the fabricated composites is neglected due to the estimation is very small.

Testing and Characterization

Surface Morphology and Crystallinity

SEM: The surface morphology was observed using scanning electron microscope (SEM, model: Emcrafts cube 2 from Korea) and the ion sputter coater (Model: Korea G20 ion sputter coater) was used for coating the samples.

FTIR: The spectral analysis was carried out using Fourier Transform Computerized Infrared Spectrometry (FTIR) (Models: FT-IR-6300, JASCO International Co., Ltd., Japan) via ATR method and recorded from 400 to 4000 cm^{-1}.

XRD: The diffraction patterns were obtained using an X-ray diffractometer (Bruker, D8 Discover) with Ni-filtered Cu-Kα radiation at with 30 mA and recorded over the range from 5 to 50 ° with a speed of 5 °/min.

Mechanical Test

Tensile Test: The tensile test was performed according to ASTM D3039 standard (rectangular shape specimen with the dimensions of 250 × 25 × 4 mm) using universal testing machine (Model: UTM-M (RB301), load cell: 100 kN, MTS System Corporation, Korea (branch), USA), with a cross head speed of 1 mm/min.

Flexural Test: The flexural test was performed according to ASTM D790 standard (rectangular shape specimen with the dimensions of 65 × 12.7 × 4 mm). The span length was taken with respect to 16 times of the thickness (16T). The test was carried out using a universal testing machine (model: UTM-M (RB301), load cell: 100 kN, MTS System Corporation, Korea (branch), USA).

Impact Test: The impact test was conducted on an Izod impact testing machine (model QC-639 F (Cometech, Korea)) with a capacity of 22 joules. The test was conducted according to ASTM D256 with a specimen size of 63.5 × 12.7 × 4 mm.

Thermal Analysis

TGA: The thermal analysis was carried out using Thermogravimetric analyzer (TGA) Q600 (TA Instruments) with a temperature ranges from 30 to 700 °C and heating rate of 20 °C/min under inert atmosphere (N_2).

Dynamic Mechanical Analysis (DMA): DMA test was carried out using Dynamic mechanical analyzer (TA Instrument Inc. Q800 v20.6 Build 24) with three-point bending mode to obtain storage modulus, loss modulus, and tan Δ as function of temperature. The experiment was conducted according to ASTM D5418 and the frequency of 1 Hz. The test was conducted from room temperature to 250 °C at a heating rate of 2 °C/min and nitrogen flow of 50 mL/min. The samples were prepared with typical dimensions of 60 × 13 × 4.5 mm^3.

Results and Discussion

Characterization of ENCVK Composites

Morphology

SEM was used to examine the morphology of the nano-cellulose-reinforced composites. Figure 1 shows SEM images of kenaf fibers (untreated and treated), vinyl ester, ENC, and commercial nano-cellulose. The figure shows that the surface of the kenaf fibers treated with the 2% NaOH solution became rough because the treatment chemicals removed the impurities and some weakly bound compounds (hemicellulose and lignin), thereby improving the mechanical and thermal properties of the fibers. The cured VE resin presented a smooth surface without any impurities, but several irregular particles were observed on the surface that may be cured VE resin particles that occurred during the specimen preparation. As explained in the previous study, the morphology of the ENC, produced using the optimized percentage of alkali and acid, almost did not resemble that of CNC, and the size with respect to length varied with a diameter of approximately 300–500 nm (magnification of 2 µm) and length approximately 3–7 µm [19]. As expected, the ENC was almost regular in shape, with a size range of 2–6 µm.

Figure 2 shows SEM images of the tensile-fractured VK, ENCVK, and CNCVK composites. Figure 2 shows that the fibers were evenly arranged, the fracture was brittle, and the fibers were pulled out, typical of the extensive

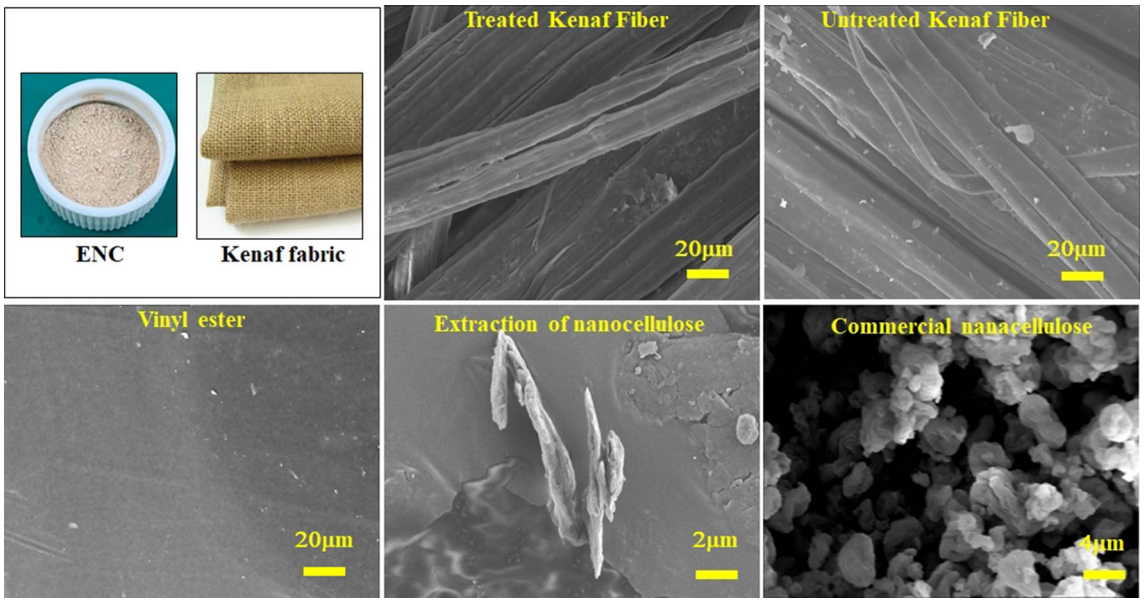

Fig. 1 Digital images of the ENC and kenaf fibers and SEM images of treated kenaf fibers, untreated kenaf fibers, vinyl ester, and the extraction of nano-cellulose and commercial nano-cellulose

fiber-to-matrix debonding that occurs before fiber failure. Different morphologies were observed for the VK- and NC-loaded VK composites. The adhesion of the two matrices of the commercial cellulose-reinforced composite (CNCVK) and ENC-reinforced composite (ENCVK) completely differed. ENC exhibited good adhesion to the vinyl ester matrix than kenaf fiber as can be observed in the pulled-out fibers appeared on the fracture surface were very clean. The SEM image and variation in mechanical along with thermal data show that the reinforcing material (NC) was uniformly distributed in the matrix. Thooyavan et al. found that different failure phenomena occur, such as fiber breakage, fiber pull-out from the matrix, matrix voids, and matrix cracks, as well as fiber breakage of the filler due to its inability to withstand the load, resulting in its transfer to the matrix [23].

Table 1 Distribution of various functional groups

Major absorption bands	Functional groups	Movement
3391	OH	Stretching
2921	sp^3CH	Stretching
1720	C = O	Stretching
1604	NH	Bending
1507	C = C (aromatic)	Stretching
1236	C–O (acyl)	Stretching
1179	C–O (alkoxy)	Stretching
1033	C–O (alkoxy)	Stretching
827	sp^2CH	Bending
757	sp^2CH (aromatic)	Bending
698	sp^2CH	Bending

Chemical Structural Analysis

Figure 3 shows the FTIR spectra of CNC, ENC, VK, ENCVK, and CNCVK, Table 1 shows the distribution of the various functional groups. From the figure, the vinyl ester exhibited spectral peaks at 3400, 2800–3000, 1713, and 1647 – 1038 cm^{-1}, corresponding to the stretching vibration of the OH groups, stretching vibration of the CH groups (CH_2 and CH_3), the carboxyl group of ester, and stretching and bending vibration of the vinyl group, respectively [24]. Figure 3A shows that the absorption bands of ENC were identified as follows: the peaks observed in the wavenumber range of 3600–2700 cm^{-1} are characteristic of O–H and C–H bond vibrations in stretched cellulose compound. The broad peak at 3391 cm^{-1} is characteristic of the vibration of the hydroxyl group in the stretched polysaccharide, further explaining the intermolecular and intramolecular hydrogen bond vibrations in cellulose. The band at 2921 cm^{-1} was attributed to the CH stretching vibration of all the hydrocarbon components in the polysaccharide. In Fig. 3B and C, typical cellulose bands of ENC occur at 1700–900 cm^{-1}. The absorption bands at 1720, 1236, 1179, and 1033 cm^{-1} were attributed to the stretching and bending vibrations of the C = O, C–O (acyl), and C–O (alkoxy) bonds in cellulose, respectively. Figure 3 shows the spectral difference between the three composite materials (VK, 4% ENCVK, and 3% CNCVK). The broad peak at 1720 cm^{-1} corresponds to the vibration of the C = O bond in the carbonate ion (CO_3^{2-}) impurity present in ENC extracted from paper egg trays usually prepared paper pulp consists of external compounds.

In 4% ENCVK spectra, the absorption band at 3600–3100 cm^{-1} (Fig. 3) was attributed to the OH vibration mode, which can be observed in almost all cellulose compounds. The results in Fig. 3 show that by combining the primary and secondary absorption bands (peaks), the ENC had functional groups equivalent to those of

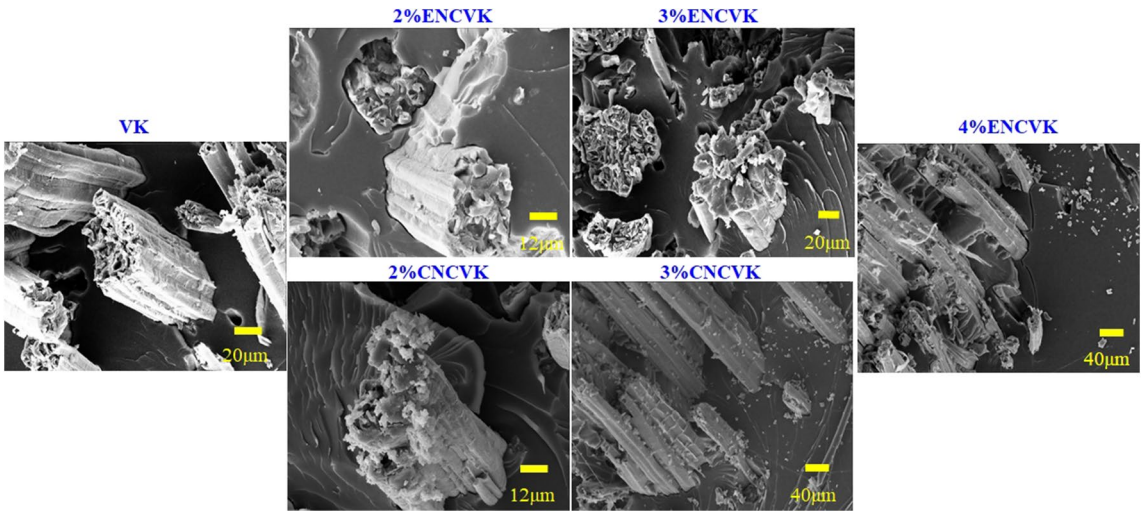

Fig. 2 SEM images of the VK, and different ratios of ENC and CNC loaded composites

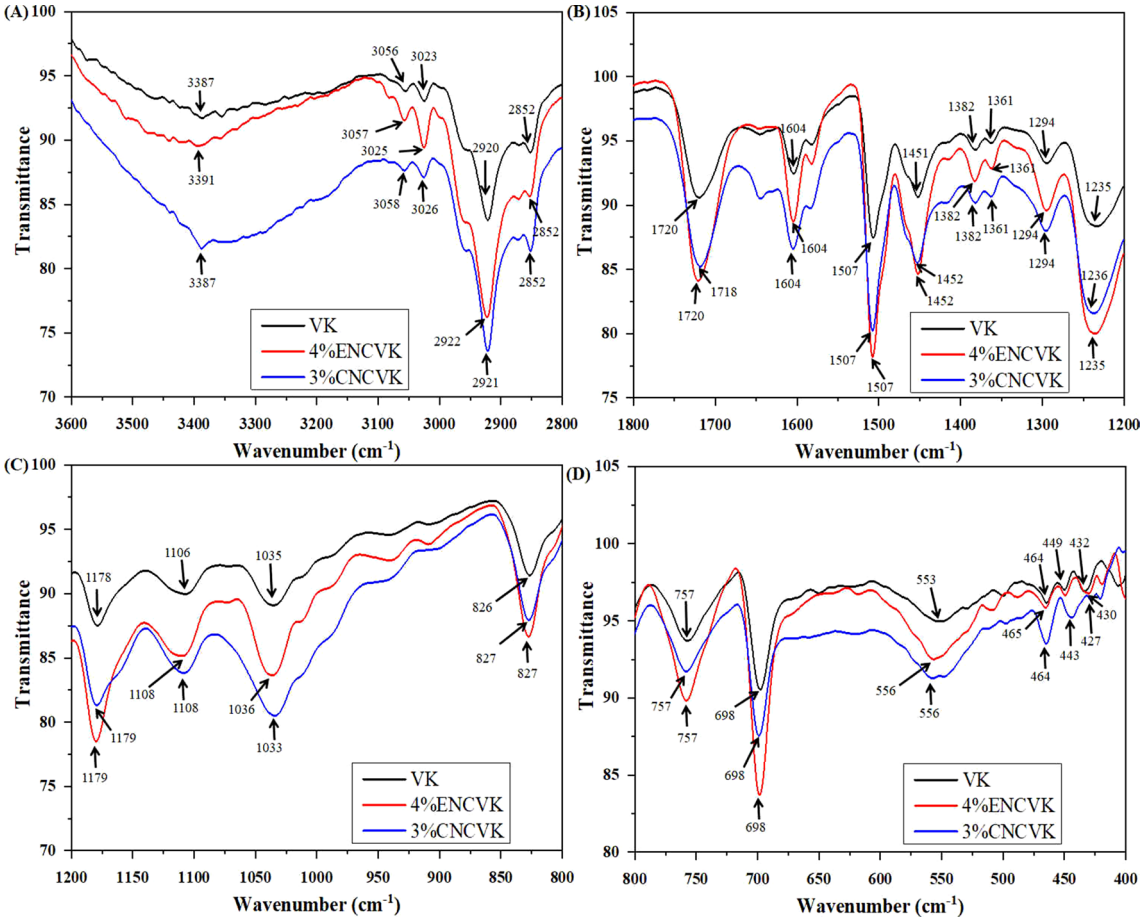

Fig. 3 FTIR spectra of VK, 4% ENCVK, and 3% CNCVK

commercial nano-cellulose. The ENC peaks at 1200–1500, 800–1200, and 400–800 cm^{-1} were stronger due to C = C (aromatic), C–O (acyl) and C–O (alkoxy) functional groups. The appearance of a new spectral peak at 3472 cm^{-1} to the chemical interaction of ENC with VK composites. Therefore, the similarity of the absorption bands (broadness of the peaks) in the fingerprint region (400–1200 cm^{-1}) supports this hypothesis. Further research is required to accurately determine the compounds highlighted by these peaks.

XRD Analysis

Figure 4 shows the XRD patterns of the ENCVK composites with different ratios. The five materials were vinyl ester kenaf fiber composite materials, which were added to the vinyl ester kenaf fiber composite materials extracted from nano-cellulose (1, 2, 3, and 4%) and vinyl ester kenaf fiber composite. Two strong peaks at 16–17° and 22–23°, which are the previously mentioned crystallinity conditions of the cellulose, were observed in all five samples [19]. The VK composite reinforced with 2% nano-cellulose exhibited the highest peak value, which led to the best performance,

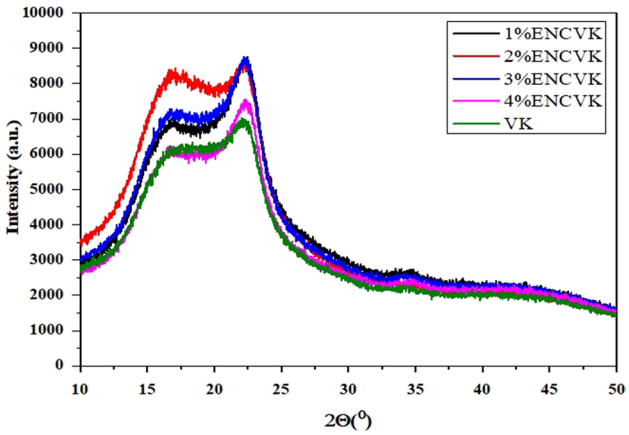

Fig. 4 XRD patterns of the VK and ENCVK composites with different ratios

followed by the 3%, 1%, and 4% reinforced ENC. Abraham et al. showed that the peaks with the nano-cellulose addition were stronger than those of the composites without the nano-cellulose addition, suggesting that increasing the

Table 2 Tensile and flexural properties of the NCVK composites

Nano-cellulose content (%)	Tensile strength (MPa)	Tensile modulus (GPa)	Flexural strength (MPa)	Flexural modulus (GPa)
VK				
0	18.655	2.875	61.283	3.481
ENC				
1%	22.225	2.565	68.254	3.610
2%	27.111	2.748	77.047	4.187
3%	32.422	3.601	67.833	4.333
4%	28.541	3.433	60.708	3.853
CNC				
2%	26.997	3.397	68.397	4.443
3%	36.191	3.461	52.392	3.493

nano-cellulose content can increase the overall mechanical properties of the composite [25].

Mechanical Behavior

Tensile Performance

A stress/strain curve reflects the relationship between the amount of stress applied to a material and the strain (or elongation) developed by the material. Figure 5 shows that a linear curve developed during tensile loading of all NCVK composite. The curve exhibits a gradual transition from the elastic to the plastic zone as shown in figure. The ENC and CNC exhibited no obvious elastic behavior on the stress-strain curves of the composites, because of thermoset matrix VE, the composite exhibited brittleness. Additionally, owing to the extensibility of natural fibers (kenaf fibers), the composite materials generally exhibited brittleness in the matrix. Under a tensile load, the material broke completely. Fiber and NC were added to the matrix to achieve overall strength that affected the overall performance of the composite material. The elongation at break values of 1% ENCVK, 2% ENCVK, 3% ENCVK, 4% ENCVK, 2% CNCVK, and 3% CNCVK are 1.17, 0.99, 1.15, 1.06, 0.95, and 1.17, 0.99, 1.15, 1.06, 0.95, and 1.44 respectively further supported the material properties. The yield strengths were 22.54, 27.20, 33.73, 28.62, 27.46, and 36.40, and that of VK were only 0.78 and 19.80, respectively. The data indicates that ENC enhanced the tensile strength of VK composites. However, the enhancement increased gradually up to 3 wt%, and a decrease was observed at 4 wt%. Because, the increase in the filler content will cause the adjacent molecular chains of nanocellulose to be subjected to greater pressure, because the tension of adjacent molecular chains increases with the increase of the percentage of filler, and the matrix withstands reaching the limit of rupture as the tensile force increases. The tensile strength of CNCVK increased with the maximum elongation. The optimized percentage of ENC for the best tensile properties was 3%. Importantly, a bonding interaction was formed between the NC and matrix, which

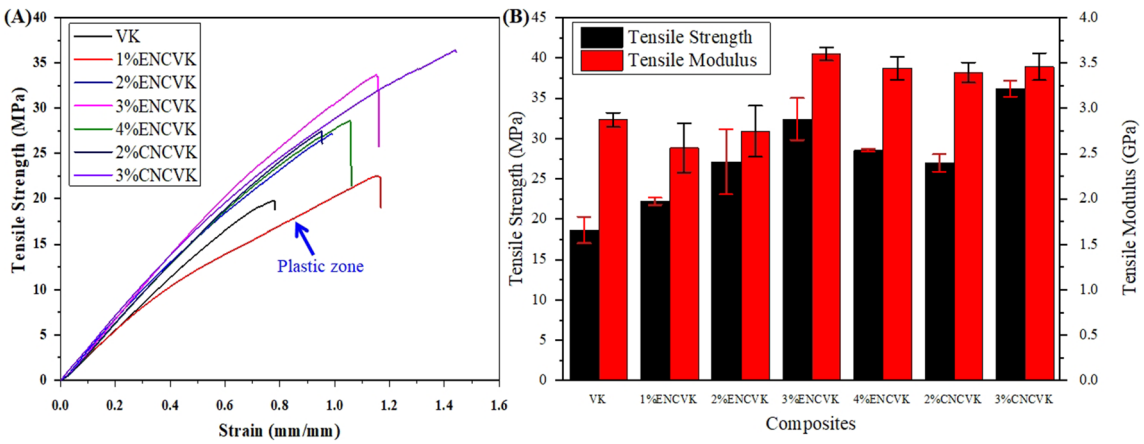

Fig. 5 Tensile performance of the different % of nanocellulose loaded VK composites

increased the tensile strength by resisting the easy formation of stress concentration points and by transferring the stress propagation during tensile loading. On average, the general trend of the stress-strain behavior of the ENCVK composites was similar to that of CNCVK.

The data obtained from the tensile test can be used to determine the tensile strength, elastic modulus, elastic limit, elongation, proportional limit, area reduction, yield point, yield strength, and other tensile performance indicators of the material. Table 2 lists the tensile properties of the NCVK composites and the standard deviations data as supplemented in the SI-Table 1. Figure 5A shows the tensile performance of the different NCVK composites. Figure 5B shows a histogram of the tensile strength and tensile modulus of the different NCVK composites. The curve exhibits a gradual transition from the elastic to the plastic zone. On average, the overall trend of the stress-strain behavior of the ENCVK composites was similar to that of the CNCVK composites.

Figure 5; Table 2 show that the tensile properties of the ENCVK composites increased with an increasing ENC content. The ENCVK composites exhibited the highest tensile strength at an ENC content of 3%. In contrast, the ENCVK composites exhibited the lowest tensile strength at an ENC content of 1%. The tensile strength of the 3% ENCVK composite was 32.422 MPa, which is 50.93% higher than that of the 1% ENCVK composite and 73.79% higher than that of the VK composite. However, when the ENC content exceeded the critical limit of 3%, the tensile strength of the ENCVK composite decreased. Table 2 shows that the tensile strength of the 4% ENCVK composite was 28.541 MPa, which is 11.97% lower than that of the ENCVK composite with a 3% ENC content. The decrement in higher % of ENC loadings may be because of the reinforcement of ENC couldn't come into effect when the failure strain of the matrix is much greater than that of the ENC. In addition, agglomeration and non-uniform distribution of ENC may play a vital role for decreasing the modulus and strength of ENCVK composites [26]. Therefore, the 3% ENC loading is an optimized percentage for obtaining tensile properties of VK composite.

A comparison of the tensile modulus of the NCVK composites with different nano-cellulose contents shows an obvious change in the tensile strength. With an increase in the ENC content, the tensile modulus of the ENCVK composite material first increased and then decreased. The 3% ENCVK composite exhibited the highest tensile modulus. When the ENC content reached 4%, the tensile modulus of the ENCVK composite decreased. The tensile modulus of the ENCVK composite with a 3% ENC content was 3.601 GPa, which was 25.22% higher than that of the VK composite. However, when the ENC content was 1%, the tensile modulus of the ENCVK composite was still the lowest of all the contents. The tensile modulus decreased with an increase in the nano-cellulose content, which was due to the decrease in the mobility of the matrix during the stretching process.

The tensile properties of the CNCVK composites exhibited similar characteristics. When the CNC content increased from 2 to 3%, the tensile strength of the composites increased by 34.05%. Table 2 shows that the tensile modulus of the CNCVK composites increased with an increase in the CNC content. The tensile strength of the CNCVK composites was higher than that of the ENCVK composites may be due to the regular shape of CNC. Moreover, the tensile strength of the CNCVK composite with a 3% NC content was 11.63% higher than that of ENCVK composite, and the tensile modulus of the 3% CNCVK composite was 4.05% lower than that of the 3% ENCVK composite material.

Flexural Performance

Similar to the tensile stress-strain behavior, increasing the nano-cellulose volume fraction increased the flexural stiffness of each composite specimen. The upper portion of the composites specimen during flexural loadings exhibited no obvious trend. The elongation of the nano-cellulose composites first increased and then decreased with an increasing fiber loading, which may be due to the stacking of the matrix with an increasing fiber content. The flexural stress-strain behavior further demonstrates that ENCVK, a predominantly brittle and hard composite, failed abruptly at the maximum point without deformation before fracture. All composites, except for the 4% ENCVK and 3% CNCVK composites, exhibited superior tensile and flexural properties, as compared to their pure matrices, indicating good compatibility between the nano-cellulose and matrix. The enhanced mechanical properties of the composites were attributed to the incorporation of the high-modulus nano-cellulose into the polymer matrix, which improved the energy absorption capacity [27]. The flexural modulus of all composites increased steadily with an increasing nano-cellulose loading, which may be due to the strong interfacial bonding between the fibers and the matrix. Therefore, the efficiency of the stress transfer increased, leading to improved mechanical properties.

Figure 6A shows the flexural test results of the different NCVK composites. Figure 6B shows a histogram of the flexural strength and flexural modulus. Table 2 summarizes the flexural properties of the NCVK composites.

The flexural strength and modulus determine the ability of the composites to resist bending loads and deformation before breaking. The overall trend of the flexural properties of the ENCVK and CNCVK composites differed from their tensile behavior. The ENCVK composites exhibited the highest flexural strength at 2%. Additionally, the 4% ENCVK and 3% CNCVK composites exhibited the lowest

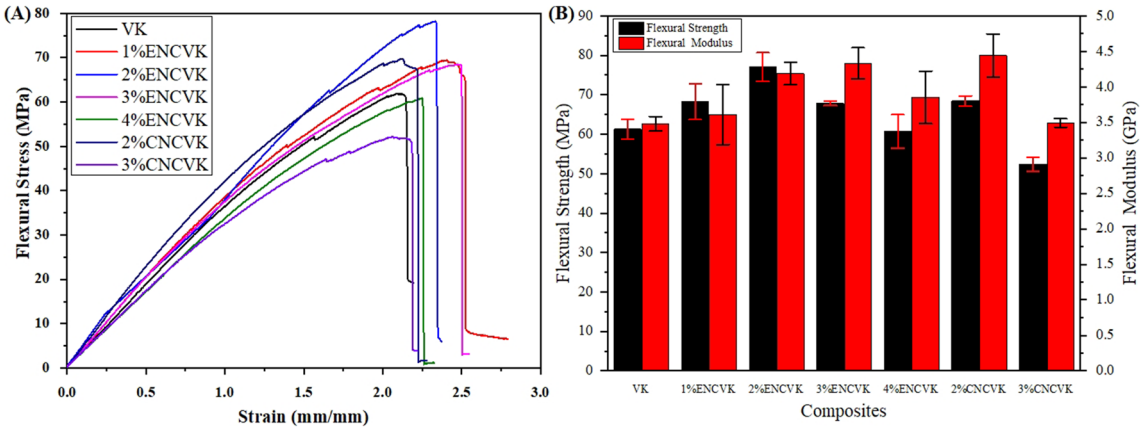

Fig. 6 Flexural performance of the different % of nanocellulose loaded VK composites

flexural strengths. Table 2 shows that the flexural strength of the ENCVK composites improved by 12.88% when the NC content increased from 1 to 2%. When the NC content increased from 2 to 4%, the flexural strength reduced by 11.96 and 10.50%, respectively. Nevertheless, any further increase in the NC content above 2% resulted in a decrease in the flexural strength of the composites. An excess NC content led to an insufficient polymer matrix which retarded the stress transfer between the NC and polymer matrix, leading to a decrease in the flexural strength [28]. These trends indicate that a NC content of 2% was optimal for the flexural strength of ENCVK composites. According to the influence of the type of NC on the flexural strength of the composites, when the same content of NC is added, the flexural strength of ENCVK composites is higher than that of CNCVK composites. Due to the rougher morphology of ENC than CNC, the bonding between ENC and VE matrix is stronger as discussed in the FTIR section described the strong bonding between ENC and matrix.

The flexural modulus of the composite materials increased with an increasing ENCVK and CNCVK content. A NC content of 3% exhibited the highest flexural modulus regardless of the ENC content. An ENC content of 4% and a CNC content of 3% in the ENCVK and CNCVK composites, respectively, resulted in the lowest flexural moduli. In the ENCVK composites, the flexural modulus at an ENC content of 3% was 20.03% higher than at an ENC content of 1%. In contrast, the flexural modulus of the CNCVK composite decreased by 21.38% when the CNC content was increased from 2 to 3%. On average, the flexural moduli of the ENCVK composites were superior to those of the CNCVK composites. Figure 6 depicts the stress/strain curves of the ENCVK and CNCVK composites with different NC contents as obtained from a 3-point bending test. The stress/strain curves of the ENCVK and CNCVK composites showed nonlinear characteristics, regardless of the NC composition. The initial stage of the curves increased linearly up to the maximum point before the stress started to decrease. The decrease in the flexural stress indicates the breaking point of the composite materials.

Impact Performance

Figure 7 depicts a histogram of the impact energies of the different NCVK composites. The 2% ENCVK composite exhibited the highest enhancement in impact strength among all the reinforcement contents, whereas the impact strength of the 3% CNCVK composites was the lowest. In contrast, the impact strength values of the other composite materials, except for the 2% ENCVK composite, differed from those of the 2% ENCVK composite materials. The impact strength of the 2% ENCVK composite was 109.98, 46.62, and 128.36% higher than that of the VK, 1% ENCVK, and 2% CNCVK composite materials, respectively. Figure 7

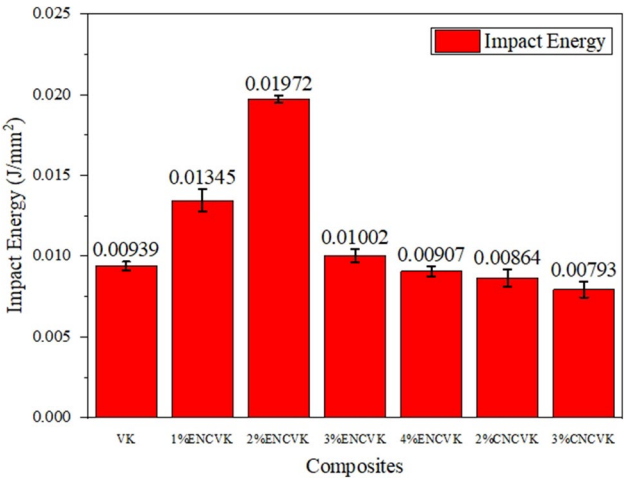

Fig. 7 Impact energy histogram of the different NCVK composites

shows that the impact performance of the 2% ENCVK composite was noticeably higher than that of the other composites in the following order: 2% ENCVK > 1% ENCVK > 3% ENCVK > VK > 4% ENCVK > 2% CNCVK > 3% CNCVK. The decrement in impact energy for higher loading of ENC because of the high content of NC will accelerate the crack propagation, transfer through the NC boundary, and reduce the time passing through the matrix. 2% ENCVK optimizes the matrix and ENC to bonding well, which slows down crack propagation and absorbs more impact energy. In particular, the ENC in the composites effectively supported the absorption of impact energy (during impact loadings initially the composite starts crack formation which can be delayed and prolog the crack propagation by nano-cellulose inclusion thereby increase the impact energy absorption). However, due to the large difference in the volume fraction of NC, when a certain content is reached, cellulose will agglomerate, resulting in poor interfacial adhesion between NC and matrix, and the overall impact energy decreases.

Thermal Analysis

Thermogravimetric Analysis (TGA)

TGA measures the variation in the weight of the composite materials with temperature or time, and determines the pyrolysis temperature, absorbed moisture content, decomposition residues, and other related information of the components in the composite material. TGA can determine the thermal stability and oxidation stability of materials in different atmospheres and can quantitatively analyze the composition of materials. Figure 8 shows the TG curves of (A) NCVK composites, (B) CNC, ENC and VE, and (C) treated kenaf fibers and untreated kenaf fibers. Table 3 lists specific data for the seven materials. After the initial moisture in VK disappeared, the mass loss of VK began to depolymerize at 250–375 °C, where the mass loss was 18.699%. The 1% ENCVK composite began to depolymerize with fluctuations in quality at 200–370 °C. The change and mass loss were 17.092%.

The 2%, 3%, and 4% composites showed similar behaviors to the 1% ENCVK and VK during the depolymerization process at 200–370 °C, and the mass losses were 19.226,

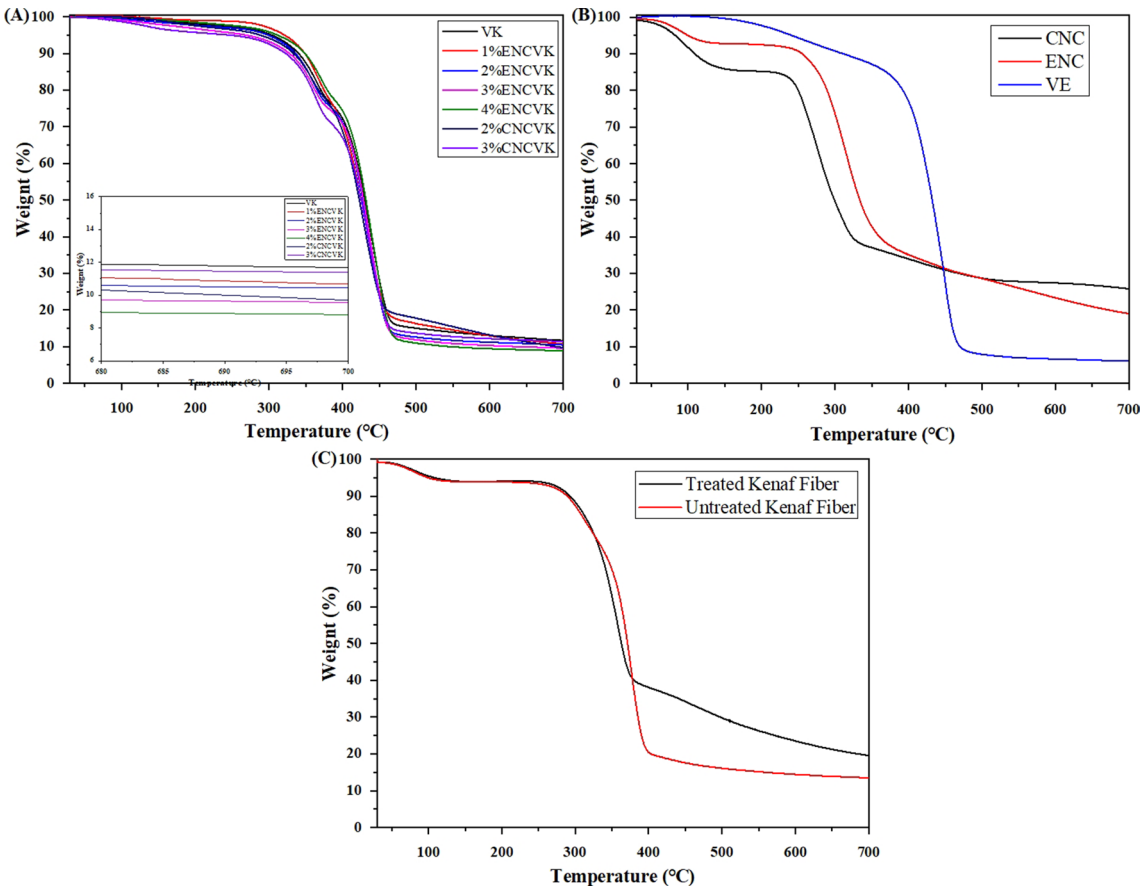

Fig. 8 TG curves of different **A** NCVK composites, **B** CNC, ENC, and VE, and **C** treated kenaf and untreated kenaf fibers

Table 3 Summary of the TGA data

Materials	T10 (℃)	T25 (℃)	T50 (℃)	T80 (℃)	@700 (wt%)
VK	340	390	430	459	11.67
1% ENCVK	348	390	425	458	10.67
2% ENCVK	336	386	427	454	10.44
3% ENCVK	327	380	428	454	9.56
4% ENCVK	349	398	432	457	8.81
2% CNCVK	334	386	423	456	9.69
3% CNCVK	322	370	425	454	11.38

19.413, and 15.107%, respectively. The depolymerized VK gradually decomposed at 375–700 °C, the mass loss was 66.855%, and the residue was 11.672% of the total mass. The 1% ENCVK composite underwent a fluctuating decomposition process at 370–700 °C, with a mass loss of 71.292% and a residue of 10.673%. At 370–700 °C, the decomposition process of the 2%, 3%, and 4% ENCVK composites was similar to KV and 1% NKV. From Table 3, the mass loss was 68.028, 67.802, and 74.601%, and the residue was 10.44, 9.563, and 8.814%, respectively. The properties of the 2% CNCVK and 3% CNCVK composites were similar to the materials described.

Figure 8 shows that as the addition of nano-cellulose increased, the thermal stability (% of char residue at 700 °C) of the composite material decreased. The TGA curve formed at the different stages of the composite material indicates that two stages of weight loss occurred at 30–700 °C. In the first stage, a slight weight loss occurring at 100–150 °C was due to the loss of residual moisture in the material. The second stage at 370–700 °C removed organic matter. The results showed that the thermal decomposition of amorphous cellulose started earlier at low temperatures but at a slower rate and ended quickly at high temperatures (370 °C). It is well known that cellulose is a semi-crystalline polymer composed of crystalline and amorphous regions. In the crystalline region, the cellulose molecules are arranged uniformly and orderly, with intramolecular and intermolecular hydrogen bonds (H bonds). In the amorphous region, the hydrogen bond network is loose and disordered, with fewer hydrogen bonds, and H bonds can form fibers which do not decompose during the pyrolysis process, significantly affecting the formation of reaction intermediates and the formation of pyrolysis products [29, 30]. Therefore, Fig. 8 shows that the performance of extracting nano-cellulose at 0–450 °C is better than that of commercial cellulose. Figure 8 shows that the mechanical properties of the treated kenaf fibers are significantly better than those of the untreated kenaf fibers.

Dynamic Mechanical Analysis (DMA)

DMA was performed to evaluate the effect of the nano-cellulose and kenaf fibers on the viscoelastic properties of the composites. Figure 9 shows the storage modulus, loss modulus, and tan Δ of VK, and the 1 and 3% ENCVK composites.

Storage modulus The storage modulus is the ratio of the in-phase stress to the applied oscillating strain, and measures the energy stored per cycle of deformation related to the elastic portion, which is closely related to the load-bearing capacity of a material [31]. A considerable improvement in the storage modulus of all the ENCVK composites was observed, which can be attributed to the introduction of rigid filler particles into the matrix phase. The storage modulus was found to be highest for the 3% ENCVK composite (3734 MPa), followed by the 1% ENCVK composite (3400 MPa) and VK (3356 MPa). Throughout the temperature range, the storage modulus values of the NCVK composites were very large and higher than that of VK. The storage modulus decreased at higher temperatures (plastic regions). However, the NC-filled composites exhibited a higher storage modulus than VK owing to the higher stiffness of the NC crystals and the better dispersion of NC in the VE matrix which produces a more rigid interface [32]. The storage moduli of the ENCVK composites were similar across the temperature range, but higher than that of pure VK, and the storage moduli decreased at higher temperatures (plastic zone). However, because of the higher stiffness of the ENC particles, their storage modulus was higher than that of VK, whereas ENC was better dispersed in the VE matrix, making the interface more rigid.

Loss Modulus The loss modulus (E'') provides the viscous response of the composites with respect to the temperature. It was observed that the loss modulus initially increased with an increasing temperature up to a certain point, and then decreased at higher temperatures. E'' depends on the type and quantity of the reinforcement. The three composites, namely VK, 1% ENCVK, and 3% ENCVK, achieved a maximum loss at 83, 122, and 110 °C, respectively, and the loss moduli were 319.1, 332.4, and 385.2 MPa, respectively. The loss modulus curves for the ENCVK composites were slightly broader than that of VK. The E'' for VK started to decrease slightly earlier than the other composites, which reflects less interaction between the filler and the matrix. The loss modulus is attributed to the slight increase in the rigidity of the composites resulting from some interfacial interaction between NC, kenaf fiber, and VE; however, it is only marginal [32]. The peak temperature of ENCVK was significantly higher than that of VK, indicating that the interfacial interaction of NC, kenaf fibers, and VE was strong, whereas the 3% ENCVK composite exhibited a superior performance.

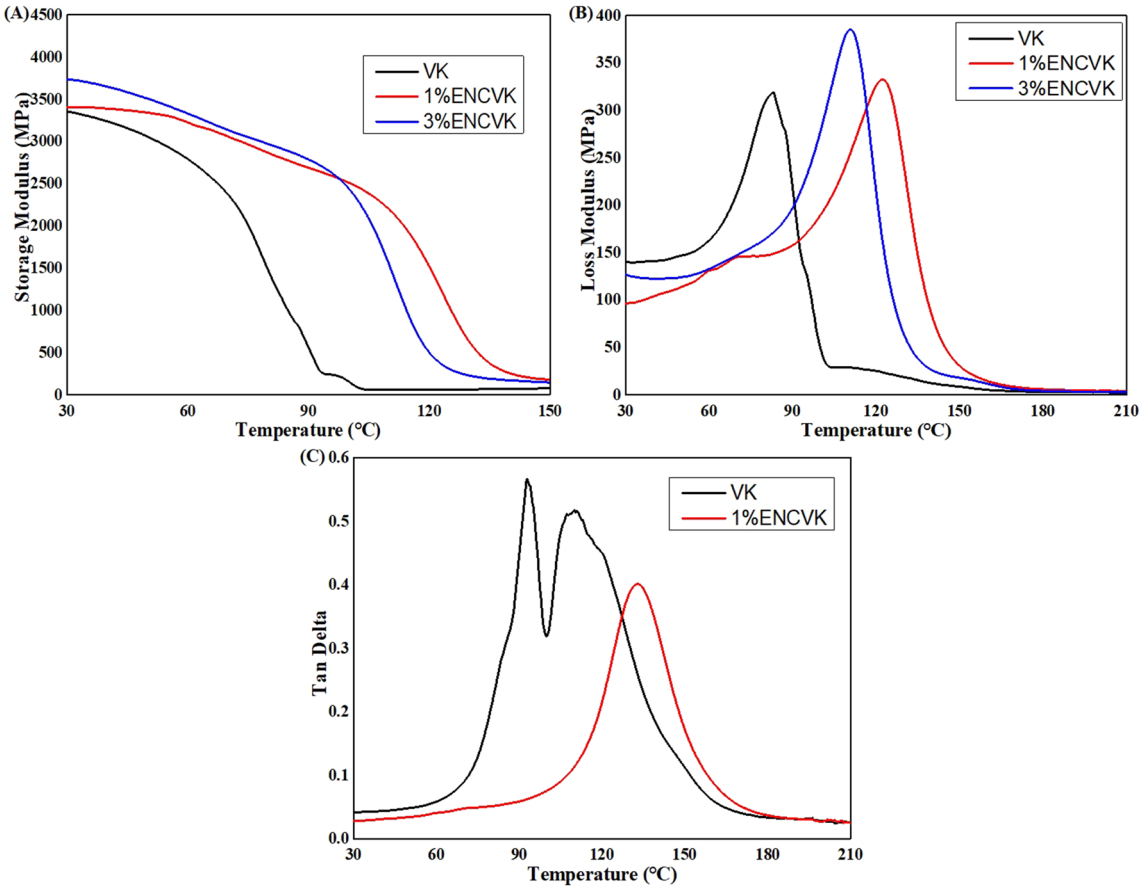

Fig. 9 DMA results: **A** storage modulus, **B** loss modulus, and **C** damping factor (tan **Δ**)

Tan Δ The ratio of the loss modulus to the storage modulus is known as the damping factor (tan Δ). The incorporation of fillers or fibers into the matrix affects the damping behavior of the composites. The damping factor of the composites changes because of stress concentrations due to the filler and viscoelastic energy dissipation in the matrix. The value of tan Δ depends on the quantum of the filler/matrix adhesion. Therefore, weaker filler/matrix adhesion will result in higher tan Δ values. If adhesion is good, the mobility of the polymer chains is reduced, which reduces damping. A low tan Δ value indicates that a specific composite has good load-bearing capacity. VK exhibited two peaks at 93 °C, peaking at 0.57, and the 1% ENCVK composite peaked at 0.40 at 133 °C. From Fig., it is apparent that the damping peaks of the ENCVK composites exhibited a small decrease in the tan Δ magnitude, as compared to VK, but the damping factor values of all the ENCVK composites were similar. The tan Δ peak of the nano-cellulose-reinforced composite was significantly smaller than that of VK, indicating that ENCVK has an excellent load-carrying capacity, and the peak temperature was higher than that of VK.

Conclusion

ENC from local bio-waste paper egg trays was successfully incorporated into the VE matrix through mechanical mixing, and manufactured VK composites by reinforcing kenaf fabrics through VARTM process. Morphological, spectral and XRD analysis concluded that the homogeneous distribution of ENC in the VE composite, change in the % of transmittance of spectral peaks and increased the intensity of the diffraction peaks respectively. The 2 wt% of ENC is the optimum loading for obtaining the maximum tensile (32 MPa), flexural (77 MPa), and impact strength (0.0197 J/mm^2) of the VK composites. Based on the thermograms of the ENCVK composites, in addition to the accelerating depolymerization process due to the presence of nano-cellulose, lower thermal stability (8 wt% char residue @ 700 °C) was achieved at a higher nano-cellulose amount. The DMA results also supported the mechanical properties, and the ENC inclusion increased the storage modulus and solid interfacial interaction with the VK composites. In conclusion, the ENC from waste paper egg trays promisingly enhanced the mechanical properties of VK composites and could replace the expensive commercial nano-cellulose.

Supplementary Information The online version contains supplementary material available at https://doi.org/10.1007/s10924-022-02588-x.

Author Contribution YR: Conceptualization, Writing—original draft, Writing—review & editing. PMN: Methodology, Validation & review. SJIL: Supervision. All authors read and approved the final manuscript.

Funding This work was supported by Basic Science Research Program through the National Research Foundation of Korea (NRF) funded by Ministry of Science Education (2018R1A6A1A03024509 and 2021R1A2B5B03002355).

Data Availability There is no data available.

Declarations

Competing interest The authors declare they have no fanatical interest.

5. References

1. Morales-Méndez JD, Silva-Rodríguez R (2018) Environmental assessment of ozone layer depletion due to the manufacture of plastic bags[J]. Heliyon 4(12):e01020
2. Ramamoorthy S, Ramamoorthy S (1997) Chlorinated organic compounds in the environment: regulatory and monitoring assessment [M]. CRC Press, Boca Raton
3. Ebitsubo H, Horie Y, Ikeda T et al (2020) Method for producing cellulose nanofiber using almond seed coat. US Patent Appl 16/506:185
4. Hussin FNNM, Attan N, Wahab RA (2020) Extraction and characterization of nanocellulose from raw oil palm leaves (*Elaeis guineensis*). Arab J Sci Eng 45(1):175–186
5. Theivasanthi T, Anne Christma FL, Toyin AJ, Subash CB, Gopinath, Ramanibai Ravichandran (2018) Synthesis and characterization of cotton fiber-based nanocellulose. Int J Biol Macromol 109:832–836
6. Sangeeta Sankhla HH, Sardar S Neogi (2021) Greener extraction of highly crystalline and thermally stable cellulose micro-fibers from sugarcane bagasse for cellulose nano-fibrils preparation. Carbohydr Polym 251:117030
7. Kumar R, Kumari S, Rai B et al (2020) A facile chemical approach to isolate cellulose nanofibers from jute fibers. J Polym Environ 28:2761–2770
8. Dongre RS (2020) Reinforce fabricated nano-composite matrixes for modernization of S & amp; T in new millennium. Composite and nanocomposite materials-from knowledge to industrial applications. InTech, London
9. Aziz T, Fan H, Zhang X et al (2020) Advance study of cellulose nanocrystals properties and applications. J Polym Environ 28:1117–1128
10. Li K, Mcgrady D, Zhao X et al (2021) Surface-modified and oven-dried microfibrillated cellulose reinforced biocomposites: cellulose network enabled high performance[J]. Carbohydr Polym 256:117525
11. Bangar SP, Whiteside WS (2021) Nano-cellulose reinforced starch bio composite films-a review on green composites[J]. Int J Biol Macromol 185:849–860
12. Naveen J, Jawaid M, Amuthakkannan P et al (2019) Mechanical and physical properties of sisal and Hybrid sisal fiber-reinforced polymer composites[M]. Mechanical and physical testing of biocomposites, fibre-reinforced composites and hybrid composites. Woodhead Publishing, Sawston, pp 427–440
13. Hazrati KZ, Sapuan SM, Zuhri MYM et al (2021) Preparation and characterization of starch-based biocomposite films reinforced by *Dioscorea hispida* fibers[J]. J Mater Res Technol 15:1342–1355
14. Mohammadkazemi F, Doosthoseini K, Ganjian E et al (2015) Manufacturing of bacterial nano-cellulose reinforced fiber—cement composites. Constr Build Mater 101:958–964
15. Tang L, Weder C (2010) Cellulose whisker/epoxy resin nanocomposites. ACS Appl Mater Interfaces 2(4):1073–1080
16. Wang WJ, Wang WW, Shao ZQ (2014) Surface modification of cellulose nanowhiskers for application in thermosetting epoxy polymers. Cellulose 21(4):2529–2538
17. Gan PG, Sam ST, Abdullah MF et al (2020) Thermal properties of nanocellulose-reinforced composites: a review. J Appl Polym Sci 137(11):48544
18. Ferreira FV, Pinheiro IF, de Souza SF et al (2019) Polymer composites reinforced with natural fibers and nanocellulose in the automotive industry: a short review. J Compos Sci 3(2):51
19. Yu R, Prabahakar MN, Lee DW, Song Jung-il (2021) Extraction and characterization of nano-cellulose from local waste paper egg trays. J Nat Fibers. https://doi.org/10.1080/15440478.2021.1964143
20. Prabhakar MN, Chalapathi KV, Atta URS, Jung-il S (2021) Effect of synthesized chitosan flame retardant on flammability, thermal, and mechanical properties of vinyl ester/bamboo nonwoven fiber composites. Cellulose 28(18):11625–11643
21. Chalapathi KV, Prabhakar MN, Jung-Il S (2020) Impact of surface treatments and hybrid flame retardants on flammability, and thermal performance of bamboo fabric composites. J Nat Fibers 3(2):1–13
22. Prabhakar MN, Naga Kumar C, Dong Woo L, Jung-Il S (2022) Hybrid approach to improve the flame-retardant and thermal properties of sustainable biocomposites used in outdoor engineering applications. Compos Part A: Appl Sci Manuf 152:106674
23. Thooyavan Y, Kumaraswamidhas LA, Raj RE et al (2022) Failure analysis of basalt bidirectional mat reinforced micro/nano Sic particle filled vinyl ester polymer composites. Eng Fail Anal 136:106227
24. Prabhakar MN, Song J (2020) Influence of chitosan-centered additives on flammable properties of vinyl ester matrix composites. Cellulose 27:8087–8103
25. Abraham E, Elbi PA, Deepa B et al (2012) X-ray diffraction and biodegradation analysis of green composites of natural rubber/nanocellulose. Polym Degrad Stab 97(11):2378–2387
26. Cho MJ, Park BD (2011) Tensile and thermal properties of nanocellulose-reinforced poly (vinyl alcohol) nanocomposites[J]. J Ind Eng Chem 17(1):36–40
27. Azhary T, Wildan MW (2022) Mechanical, morphological, and thermal characteristics of epoxy/glass fiber/cellulose nanofiber hybrid composites[J]. Polym Test 110:107560
28. Zaghloul MYM, Zaghloul MMY, Zaghloul MMY (2021) Developments in polyester composite materials—an in-depth review on natural fibres and nano fillers[J]. Compos Struct 278:114698
29. Jiang S, Farooq A, Zhang M et al (2022) Bionanocomposite using nanocellulose obtained from agricultural biomass[M]. Biorenewable nanocomposite materials, vol 1. Electrocatalysts and energy storage. American Chemical Society, Washington, pp 75–90
30. Taib MNAM, Hamidon TS, Garba ZN et al (2022) Recent progress in cellulose-based composites towards flame retardancy applications[J]. Polymer. https://doi.org/10.1016/j.polymer.2022.124677
31. Nagarajan V, Mohanty AK, Misra M (2013) Sustainable green composites: value addition to agricultural residues and perennial grasses. ACS Sustain Chem Eng 1(3):325–333

32. Jawaid M, Khalil HPSA, Hassan A et al (2013) Effect of jute fibre loading on tensile and dynamic mechanical properties of oil palm epoxy composites. Compos Part B: Eng 45(1):619–624